

Utilizing an Organ-on-a-Chip to Study the Introduction of a Fecal Treatment at  
Hyperthermic Conditions

Thesis

Presented in Partial Fulfillments of the Requirements for the Degree Master of Science in  
the Graduate School of The Ohio State University

By

Sean Patrick McGowan, B.S.

Graduate Program in Microbiology

The Ohio State University

2024

Thesis Committee

Karen Dannemiller, Advisor

Justin North

Joshua Hagen

Article is approved for Distribution A, public clearance, on 13 Feb 2024 under the  
originator reference number: RH-24-125354

Copyrighted by

Sean Patrick McGowan

2024

## Abstract

The human gut microbiome is the collection of the microbiota that reside in the human intestinal tract. Imbalances in the gut microbiome are associated with multiple diseases, so studying this is important for preventing and treating these conditions. These imbalances can have multiple causes, such as changes in core temperature. Previous work has indicated that the gut microbiome could play a role in mitigating negative effects of temperature on epithelial tissues, which could have profound effects on human health. Research into the human gut is normally performed by way of animal models, or by using a synthetic model involving the use of human cells on transwells. The goal of this study was to collect preliminary data to determine if gene expression in gut epithelial cells is influenced by the presence of a fecal sample at hypoxic, hyperthermic conditions. An experiment was performed on 36 gut-on-a-chips over the course of 48 hours at three different temperature levels: 30°C, 37°C, and 42°C. Next-Generation Sequencing (NGS) was performed to determine gene expression in the human epithelial cells when comparing the introduction of a fecal sample to the chip in low-oxygen conditions at 42°C. Most genes in the host cells were upregulated when exposed to the fecal sample, with the majority being involved in immune system responses, as well as cell growth and differentiation, host metabolism, and enzymatic activity, which is consistent with what would be expected when the gut bacteria are present. The gut-on-a-chip can be used to study temperature effects on the human epithelial cells, as well as test ways to counteract

any negative effects that come with this shift. Future studies can elucidate the role that the gut microbiome may play in the response of the human body to changes in core temperature.

## Dedication

This thesis is dedicated to my grandfather, David L. McGowan, who supported my studies throughout my college career, but unfortunately passed away during the production of this work.

## Acknowledgements

Words cannot express my gratitude to my thesis advisor and committee chair, Dr. Karen Dannemiller, for her invaluable support and feedback on this project. I also could not have undertaken this journey without my committee members, Dr. Joshua Hagen and Dr. Justin North, who generously provided knowledge and expertise throughout this process. I am also extremely grateful to Drs. Tyler Nelson's and Matthew Grogg's group at the Air Force Research Lab, who provided the lab space, materials, and extensive expertise and support to perform the chip experiments for this thesis. I am also deeply grateful to the other graduate student on this project, Taylor Chermak, for helping support my research all the way to the final product. Additionally, this would not have been possible without SOCHE/DAGSI, who funded my research.

I am also grateful to Drs. Seth Faith and Mike Sovic, and those at IDI-GEMS for taking me under their wing during my first year and providing knowledge on library prep, sequencing, and data analysis needed. Thanks should also go to The Ohio State Microbiology Department for their support and guidance during my work, as well as my cohort members for their editing help, late night study sessions, and moral support. Lastly, I would like to thank my parents for keeping my spirits and motivation at a high during my time at Ohio State, as well as my dogs, Boomer and Buck, for providing emotional support during the rougher periods.

Vita

May 2019.....Dublin Scioto High School

April 2022.....B.S. Biological Sciences, Bowling Green  
State University

August 2022 – August 2023 .....Graduate Teaching Associate,  
Department of Microbiology, The Ohio  
State University

August 2022 – present .....Graduate Research Associate, Department  
of Microbiology, The Ohio State  
University

## Table of Contents

Abstract.....	iii
Dedication.....	v
Acknowledgements.....	vi
Vita.....	vii
List of Tables.....	ix
List of Figures.....	x
Chapter 1: Introduction.....	1
Chapter 2: Utilizing an Organ-on-a-Chip to Study the Introduction of a Fecal Treatment at Hyperthermic Conditions .....	15
References.....	45



## List of Tables

<b>Table 1.</b> Pre-library prep concentrations are listed in ng/ $\mu$ L, as well as RNA Integrity Numbers (RINs). Sample 6 had to be diluted, as the undiluted concentration was too high for the Qubit fluorometer to read.....	30
<b>Table 2.</b> Post-library prep concentrations are listed in the third column in ng/ $\mu$ L. Concentrations of the prepped samples after the left side cleanup are in the fourth column, and the size of the library (in units of base pairs) taken from the TapeStation are in the last column.....	32
<b>Table 3.</b> DESeq2 table showing up or downregulation when a fecal sample is introduced to the chip. All 66 genes with a significance of $p < 0.01$ are listed, separated by general gene function and sorted by adjusted p-value. Adjusted p-values were generated in the DESeq2 program using the Wald test. Genes highlighted in yellow are considered to be significant based on the parameters set ( $p\text{-value} < 0.01$ , $\log_2\text{FoldChange} > 2.00$ ). Standard errors in $\log_2\text{FoldChange}$ are also listed. All values in the table have been rounded to 3 significant figures.....	36-38

## List of Figures

- Figure 1.** Graphical representation of the experimental workflow for the organ-on-a-chip. 36 chips were seeded and separated into 6 groups of 6 chips based on oxygen level and temperature. For the purposes of this paper, only the gut host cells of the 42°C hypoxic group were sequenced (Red Circles).....21
- Figure 2.** (A-G) TapeStation electrophoresis graphs of samples 1-6 and the negative control. An average bp size was estimated based on peaks and where the middle curve started and ended. (A, B) For samples 1 and 2, due to the odd shape of the curve, an average bp size of 400 was estimated for both.....33
- Figure 3.** Volcano plot showing effects of fecal treatment on hypoxic host sample gene expression. Log2FoldChange is plotted on the X-axis vs. p-value on the Y axis. Each dot represents a single gene in the human genome, and a positive log2FoldChange indicates upregulation when exposed to the fecal sample vs no fecal treatment. Blue dots represent significant up/downregulation, indicating an adjusted p-value < 0.01 and a log2FoldChange > 2.00, and red dots indicate no significance.....39

## **Chapter 1: Introduction**

In the past several years, the development of low-cost and high-throughput sequencing methods and analytical tools has allowed for extensive research into the human gut microbiome. In this chapter, we will discuss the development and role of gut microbes on human health, as well as a new way to model the gut microbiome *in vitro*. When the term “microbiome” is used in this thesis, only the bacterial component will be referred to due to its’ high abundance in the human gut and a lack of studies that relate to eukaryotes and viruses in the gut. Future studies could examine the role of other microbes, including eukaryotes.

### **The Human Gut Microbiome**

The gastrointestinal tract (GI tract) is a system that spans an area of around 250-400 m<sup>2</sup> and includes the oral cavity, pharynx, esophagus, stomach, small and large intestines, and the anus, and is used to digest and absorb food and excrete the waste products (Thursby and Juge 2017, Ogbuiro et al 2023). The human gut microbiota is a collection of microbes that are associated with the digestive tract in humans, while the human gut microbiome refers all the microbes in the human gut. The human gut microbiota is estimated to be made up of about 10-100 trillion microbes, with the vast majority residing in the colon (Ley et al. 2006); however, a study shows that the ratio of microbial cells to

human cells in the human body is closer to a 1:1 ratio, as opposed to the original ratio of 10:1 originally estimated (Sender, Fuchs, and Milo 2016). The microbiome contains over three million genes, much more than ~23,000 contained in the human genome (Valdes et al. 2018). The adult human gut microbiota is thought to mainly consist of more than 1000 species-level phylotypes of bacteria from the *Firmicutes*, *Bacteroidetes*, *Actinobacteria*, *Proteobacteria*, *Fusobacteria*, and *Verrucomicrobia* phyla, (with *Firmicutes* and *Bacteroidetes* being the dominant phyla), along with smaller relative amounts of methanogenic archaea, eukaryotes and viruses; however, while these phyla are consistent across the vast majority of microbiotas, the relative ratios of phyla and species present can be vastly different between individuals (Lozupone et al. 2012). Because bacterial species comprise much of the microbiota, most studies are focused on the bacteria, leaving the other players understudied (Hillman et al. 2017). These smaller microbes (such as bacteriophages) can still play an important role in the gut (Mills et al. 2013). Bacterial abundance and diversity also vary based on where in the gut the microbes reside. The small intestine is more acidic and has higher levels of oxygen, so the small intestine is mainly colonized by a lower density of fast-growing facultative anaerobes that can tolerate acidic environments, while the colon has a higher density of fermentative polysaccharide-degrading anaerobes that can break down the polysaccharides that pass through the small intestine (Donaldson, Lee and Mazmanian 2016). The United States National Institute of Health (NIH) has supported the Human Microbiome Project, which is a project that aimed to develop a reference dataset of isolated microbial genome sequences, profile the human microbiome, create integrative datasets from both the microbiome and hosts in people with microbiome-associated diseases and develop

computational tools to aid in studying the microbiome (Human Microbiome Project Consortium 2012). As of 2024, the HMP contains information 31,596 samples taken from 48 primary sites in the human body, and this data has contributed tremendously to the study of the human microbiome (Human Microbiome Project Data Portal).

The gut microbiota contributes to food fermentation, immune responses, production of vitamins and protection against certain pathogens. Other microbiotas are important in human health that will not be covered in this introduction, including those in the oral cavity, lungs, and skin (Hou et al. 2022). In the next section, the development of the gut microbiome from birth to adulthood will be discussed.

### **Development of the Human Gut Microbiome**

The human gut is commonly believed to be sterile at birth, despite some limited studies showing that bacteria are detected in womb tissues like the placenta (Aagaard et al. 2014). During and after birth, infants are then exposed to microbes from both their mother and the environment, which rapidly colonizes the infant's gut, and the microbiota develops into a more complex composition that resembles the adult human gut by around 1-2 years old (Ma et al. 2020). Studies show that the method of delivery can also have an effect on colonization of the neonatal gut microbiome, with one study showing that infants born by cesarean section have lower numbers of *Bacteroides* and higher numbers of *Clostridioides difficile* when compared to vaginally born infants (Penders et al. 2006), although this difference seems to disappear after about 6-12 months after birth

(Rutayisire et al. 2016). Vaginally delivered infants are also shown to gain some of their microbiota from the mother's feces, as a study shows that the same *Escherichia coli* serotypes were found in both the mother's feces and mucus extracted from the infant's mouth post-delivery (Bettleheim et al. 1974). However, it is suggested that cesarian section infants receive *E. coli* serotypes from environmental factors, such as contaminated equipment or from the nursing staff (S. Lennox-King et al. 1976). After birth, a few factors can determine the composition of the infant's gut microbiome, including the infant's diet, the use of antibiotics, and the environment around them. When the child is born, they can be fed with either breast milk or formula, which can potentially influence the abundance of certain species in the gut. In fact, a study showed that breastfeeding is associated with higher levels of *Bifidobacterium* and *Bacteroides* and lower levels of *Clostridia* species, and that alpha diversity remains unchanged before 3 months but increases significant around 6 months, corresponding with the addition of solid food in months 4-6 (Ma et al. 2020).

Antibiotic usage is another thing that can affect early gut microbial composition. A small study found that the introduction of antibiotics (ampicillin and gentamicin) within weeks of birth could significantly reduce beneficial phyla like *Actinobacteria* and some *Firmicutes*, while members of *Proteobacteria* tend to dominate even after antibiotic treatment was halted after 8 weeks (Fouhy et al. 2012). Finally, the environment plays a role in an infant's gut microbial composition. For example, infants born in Northern European countries have a higher proportion of *Bifidobacteria* than those born in Southern Europe, and Southern European infants also had a relatively more diverse

microbiota with a higher abundance of *Bacteroides* than northern infants (Fallani et al. 2010). Another example of this was a study that shows there were significant difference in gut microbial phylogeny between American, Malawian and Amerindian infants, and that Malawian and Amerindian microbial communities are more similar to one another than to the American infant's microbiome (Yatsunenکو et al. 2012). This could be due to the lifestyle and diet similarity between the Malawian and Amerindian villages, but are completely different from that of a western diet in metropolitan areas like St. Louis or Philadelphia (Yatsunenکو et al. 2012).

The human gut develops over the first few years of an infant's life, and plays an important role in the health and homeostasis of the host. In the next section, the role of the gut microbiome in the health of humans will be discussed.

### **Temperature effects on Human Health and the Gut**

The average human core body temperature is 37°C (98.6°F), with a person experiencing hyperthermia when body temperatures reach above 37.5°C (99.5°F) and hypothermia when temperatures are below 36.5°C (97.7°F). There has been a system put in place known as the Swiss system, which categorizes the stages of hypothermia based on core temperature (Pasquier et al. 2016). Stage 1 (mild) consists of consciousness and shivering with a core temperature of 35-32°C, stage 2 (moderate) consists of impaired consciousness without shivering with a core temperature of 32-28°C, stage 3 (severe) consists of unconsciousness at 28-24°C, and stage 4 has no vital signs and core

temperature below 24°C (Brugger et al. 2012). No set system exist for heat, but the general consensus splits the stages of hyperthermia into heat exhaustion and heat stroke, with the changeover at about 40°C. Cold temperatures can cause the veins and arteries in the human body to narrow, which could increase the risk of cardiovascular disease (Zhang et al. 2014). During cold stresses, the body can undergo nonshivering thermogenesis in brown adipose tissue, where the host protein UCP1 uncouples proton transport from ATP synthesis and generates heat (Li et al. 2019). The abundance of *Firmicutes* and the production of short chain fatty acids increase when the core temperature decreases, and the *Verrucomicrobia* phylum almost completely disappears under cold stress, which helps to facilitate enhanced energy extraction (Chevalier et al. 2015). Conversely, during heat stress, the abundance of *Firmicutes* and overall alpha diversity declines, and can also increase the risk of gram-negative bacterial infections and septic shock risk (Ogden et al. 2020, Schwab et al. 2014, Huus and Ley 2021).

A limited number of studies have shown temperature to influence epithelial cells. A mouse study showed that under heat stress of 42°C, epithelial damage in the gut was evident as early as 30 minutes post exposure, and significantly worsened after 60 minutes compared to a control group (Lambert et al. 2002). A later studied described a potential link between epithelial barrier integrity and the gut microbe *Akkermansia muciniphila*, as the introduction of this species before the heat stress was shown to mitigate epithelial barrier damage at 43°C (Peng et al. 2023). Both studies were performed on mouse models; however, the effects of temperature on human epithelial cells have been understudied.



## How the Gut Microbiome Affects Health

The relationship between the human gut and the bacteria harbored inside is a mutualistic one (Bäckhed et al. 2005). First, gut bacteria are involved in metabolic processes and intestinal barrier integrity. Gut bacterial enzymes are able to carry out biotransformation of bile into secondary bile acids (Lefebvre et al. 2009, Staley et al. 2017). The microbiome can also provide metabolic pathways for nondigestible substrate fermentation (things like fibers and mucus), which lead to the growth of microbes that produce short-chain fatty acids that can be useful for protecting the epithelium of the intestine, as well as stimulating absorption of salt and water in the colon (Vyas and Ranganathan, 2012). These short chain fatty acids include acetate (which is produced by most gut microbes) propionate, and butyrate, as well as other end products like lactate, ethanol, succinate, and formate, among others (Vyas and Ranganathan, 2012). Butyrate, produced mainly by *Firmicutes*, can be used to fuel colonocytes, which is a main regulator of a tight junction protein that regulates the epithelial barrier integrity (Louis and Flint 2016, Morrison and Preston 2016). Butyrate has also been shown to be anti-inflammatory by suppressing NF- $\kappa$ B (which is involved in Crohn's disease) (Segain et al. 2000), and inhibit cytokines like IL-12 and TNF- $\alpha$ . Propionate, produced mainly by the succinate pathway in Bacteroidetes, has recently been shown to reduce visceral and liver fat, inhibit *de novo* lipogenesis (DNL) and cholesterologenesis driven by acetate, and is involved in mucin degradation when produced by *A. muciniphila* and a reduction in liver cancer cell proliferation (Louis and Flint 2016, Morrison and Preston 2016, Bindels

et al. 2012). Gut bacteria like bifidobacteria have been shown to synthesize vitamin K and certain vitamin B molecules like biotin, folates, and riboflavin (LeBlanc et al. 2013).

Gut bacteria also have a role in protecting the host from pathogens and development of the immune system. Intestinal bacteria compete for nutrients and attachment sites in the gut, which is known as competitive-exclusion effect (Bull and Plummer 2014). Because of this competition, enteric bacteria can outcompete pathogenic bacteria based on the overwhelming number of enterics, and can also produce antimicrobial bacteriocins that can inhibit growth of the pathogens (Gaurner and Malagelada 2003). This is mainly done by bacterial quorum sensing, where the bacteria sense changes in the environment and adjust their phenotypes to alter motility, density, or excretion of antimicrobials (Wiertsema et al. 2021). Gut microbiota can also induce mucosal Secretory IgA, which is then anchored to the outer mucosal layer and provide protection against pathogens (as reviewed in Thursby and Juge 2017). A study done has shown that the gut anaerobe *Bacteroides fragilis* can reverse the lack of expansion of CD4+ T-cells in germ-free mice through the pattern recognition receptors of the epithelial cells, which is required for the immune system to react to infectious agents (Mazmanian et al. 2005). Another study has shown that a protein produced by *Faecalibacterium prausnitzii* can inhibit the NF-KB pathway in the epithelium and prevent colitis (Quévrain et al. 2015).

The gut has the potential to have an imbalance between beneficial and pathogenic bacteria, which could disrupt the homeostasis of the gut in what is known as “dysbiosis,” which is characterized by a loss of beneficial organisms, excessive growth of pathogenic

bacteria, or a decrease in overall microbial diversity. Microbial dysbiosis has been suggested to have associations with many diseases, such as inflammatory bowel disease (IBS), irritable bowel syndrome (IBD), obesity and type 2 diabetes. IBS is a group of disorders characterized by abdominal pain and either, diarrhea, constipation, or a mix of both, and affects 10-20% of adults in the world (Longstreth et al. 2006). While it is not known what exactly causes IBS, it has been shown that IBS patients show an increase in *Firmicutes*, while the abundance of *Bacteroidetes* is at a lower level than that of a healthy gut microbiota (Guinane and Cotter 2013). IBD is a set of two conditions (Crohn's disease and ulcerative colitis) that is characterized by inflammation of the GI tract. Both diseases are shown to have decreased bacterial diversity, with a lower abundance of *Bacteroides* and *Firmicutes*, an increase in proteobacteria, and a decrease in *F. prausnitzii*, which we have previously discussed (Chang and Lin 2016). This decrease can also affect bile acid transformation, causing less conjugation and an increase in the inflammation caused by IBD (DeGruttola et al. 2016). Obesity is a major disease that is prevalent in 41.9% of the US population in 2017 (CDC), and can cause metabolic syndrome, which further increases risk for cardiovascular disease, insulin resistance and type 2 diabetes (Mayo Clinic Staff, 2021). A lower abundance of *Bacteroidetes*, with a proportional increase of *Firmicutes* has been shown to occur in obese mice compared to lean mice (Ley et al. 2005). Short chain fatty acids have also been shown to be elevated in obese adults and children (Schwiertz et al. 2010, Payne et al. 2011). Finally, type 2 diabetes is a disease characterized by a resistance to insulin or the pancreas being unable to make enough insulin (CDC 2023). Those with type 2 diabetes have been shown to have a decreased amount in *Firmicutes* and an increase in *Bacteroidetes*, and drugs such

as metformin (which is used to treat type 2 diabetes) has been shown to alter the microbiota composition by modulating short chain fatty acid-producing bacteria, which increases butyrate and propionate production to help with gut permeability and homeostasis (Larsen et al. 2010, Iatcu et al. 2022).

Antibiotics have also been shown to be a factor in causing gut microbiota dysbiosis (Langdon et al. 2016). When given antibiotics, microbial taxa number decreases by about 25%, which can indirectly disturb beneficial microbial interactions and causes dysbiosis, and another found that antibiotics can predispose the host to more severe infections, such as *Clostridium difficile* (Panda et al. 2014, Sekirov et al. 2008). *C. difficile* infection is one of the most common and serious gut-associated infections, accounting for almost 500,000 infections in the United States in 2011, and can cause varying symptoms from diarrhea to pseudomembranous colitis and even death (Lessa et al. 2015, Yoon and Yoon 2018, Na et al. 2014). When antibiotics disrupt the microbial communities, it facilitates germination and growth of the microbe, regardless of what antibiotic is used (Mullish and Williams 2018, Britton and Young 2014).

Probiotics are microorganisms that can be administered to the gut to change composition and provide health benefits to the host. Probiotics work by inducing production of beta defensin and IgA, which suppresses the growth of pathogens in the gut (Hemarajata and Versalovic 2013). One example of this is using strains of *Lactobacillus* as a probiotic, which can decrease phenotypes of GI diseases like IBS and IBD (Lee and Bak 2011). Another study in 2016 also showed that probiotics shift gut composition, as when mice

who had hepatocellular carcinoma were given a probiotic, *Prevotella* and *Oscillibacter* were significantly increased, which produced anti-inflammatory metabolites that reduced tumor size and weight (Li et al. 2016).

The gut microbiome can protect the host from pathogens by producing metabolites that can maintain the intestinal barrier integrity and develop the immune system, but can also cause serious problems when an imbalance in microbial composition and diversity upsets gut homeostasis. In the next section, how temperature affects the gut microbiome will be discussed.

### **Models Used to Study the Human Gut Microbiome**

Studying the human gut microbiome has always been a challenge, especially when concerning ethical limitations and whether the model used is biologically relevant to humans. Some of the main ways that researchers have studied the gut microbiome is through human sampling, the use of model organisms, and through manufactured systems. When sampling humans, the most common way to study the gut microbiome is through the use of stool samples. This method has a variety of pros and cons, as it is usually non-invasive, has a high level of microbial density and low contamination, but samples need to be frozen and preserved immediately so that the samples do not get contaminated from the environment (National Academies of Sciences, Engineering, and Medicine 2017). Nonhuman models can also be used to study the gut microbiome. Animal studies are widely used to study how different variables could affect the host

microbiome, including age, diet, or based on body site, but the drawback is whether the animal study can be physiologically relevant to humans. For example, germ-free mice are one of the most common animals used in animal studies on the gut microbiome, due to the similar structure that mice have with humans in the gastrointestinal tract, but there are still some differences, such as mice lacking mucosal folds in the intestine or the lack of division in the colon (Nguyen et al. 2015). Mice and humans also have a similar gut microbial composition, as they are both dominated by *Bacteroidetes* and *Firmicutes*; however, a study done by Ley et al. found that 85% of their sequences from mice represent genera that aren't detected in humans (Ley et al. 2005). The last model type used to study the human gut is to use an engineered system *in vitro*, which is a relatively new way to study the gut that is non-invasive, has no major ethical limitations, and is biologically representative to humans. One of these models, the organ-on-a-chip system, will be discussed in the next section.

### **Applications of the Organ-on-a-Chip**

When studying the gut, the primary method of study is by using animal models; however, there is a rather major limitation to this, as animal models such as mice are unable fully to replicate human physiology, and are unable to predict responses to drugs in humans (as reviewed in Ashammakhi et al. 2020). The most common way to model the gut *in vitro* using an engineered system is to culture a human intestinal epithelial cell line on extracellular matrix in a transwell, but this also has the limitation in that it fails to capture a 3-dimensional physiological representation, along with key intestinal functions like

mucus production or drug metabolism (Bein et al. 2018). With recent advances in microfluidics and fabrication, the development of these organ-on-a-chip models allow for a system to be more closely related to the structure and physiology of the human organ it is representing (Fetah et al. 2019, Whitesides 2006, Trukillo-de Santiago et al. 2018). These chip models all have hollow microchannels that are lined with living cell tissue and separated by a membrane that can be cultured under a dynamic fluid flow, and these chips can be coupled to make body-on-a-chip models that can potentially mimic interactions between different organs, as well as whole body physiology (Ingber 2022). These modelled organs can include the lungs, intestines, heart, and brain, among others (Ingber 2022). For a few examples, a study on a lung-on-a-chip model have shown that the addition of IL-2 into the microvascular channel can induce pulmonary leakage into the alveolar channel, which mimics lung function seen in a clinical setting (Huh et al. 2012). Brain chip systems have been used to replicate the substantia nigra area of the brain in an effort to replicate Parkinson's disease (Pediaditakis et al. 2021), as well as numerous studies using brain chips to model the shuttling of molecules across the blood brain barrier (Park et al. 2019, Lee and Leong 2020, Morad et al. 2019). Intestine chips have been shown to effectively promote villi formation when undergoing dynamic fluid flow, and colon chips have been seen to generate a physiologically relevant bilayer structure of mucus that can potentially be used to show the role of mucus in homeostasis (Sontheimer-Phelps et al. 2020, Kasendra et al. 2018). Numerous studies have been done using a combination of chip systems in order to create a single platform. A study published in 2017 was able to use a combination of both a gut and liver chip, along with the drug apigenin, to reproduce the first pass metabolism of drugs (Choe et al. 2017).

Previous work has indicated that the gut microbiome can mitigate the negative effects of temperature changes on epithelial tissues, which could profoundly affect human health. This thesis work aims to collect preliminary data to determine if gene expression in gut epithelial cells is influenced by the presence of a fecal sample at hypoxic, hyperthermic conditions. Using an organ-on-a-chip model and Next-Generation Sequencing, 66 genes were found to have a significant p-value of less than 0.01, and 5 of these genes were found to be significantly upregulated ( $\log_2\text{FoldChange} \geq |2|$ ,  $\text{padj} < 0.01$ ). These results indicate that, when a fecal sample is present, the host epithelial cells significantly upregulate expression of these 5 genes in response at hyperthermic conditions. This study provides the framework to study other temperature effects on human gut epithelial cells, and could further drive research into studying gene expression due to temperature-driven changes in the gut.



## Chapter 2: Utilizing an Organ-on-a-Chip to Study the Introduction of a Fecal Treatment at Hyperthermic Conditions

### **Introduction**

Hyperthermia has been associated with many significant health issues, such as heat exhaustion and heat stroke. In 2021, there were 1,864 cases of heat exhaustion and 488 cases of heat stroke among active-duty service members in the United States, and this carries a huge financial and medical burden on the military (Armed Forces Health Surveillance Branch 2021). This heat stress has a detrimental effect on gut tissue and the endothelial barrier that could cause associated gastrointestinal diseases; however, the mechanism and extent of these effects are unknown. Previous studies have shown that certain gut bacteria (such as *Akkermansia muciniphila*) could help mitigate these negative effects on epithelial tissue (Peng et al. 2023). Because of this, one area that is of high interest is to further study the effects of the gut microbiome, and whether it could have a role in preventing epithelial barrier disruption.

Traditional methods to study the human gut include using animal models and synthetically engineered systems like the transwell. Mouse models are commonly used to study the gut microbiome, but they lack gut features common in humans like mucosal folds and a divided colon, while also still containing genera that aren't commonly in the

human gut microbiome (Nguyen et al. 2015, Ley et al. 2005). Culturing human intestinal epithelial cells in a transwell has previously been used to study things like barrier integrity and permeability related to IBD, but this method cannot model a three-dimensional physiology, as well as functions like mucosal production or drug metabolism (Gleeson et al. 2021, Bein et al. 2018). Recent advances in microfluidics have allowed for the development of organ-on-a-chip models that can more closely resemble the physiology of a human organ *in vitro*, while also replicating biological functions in the gut that could potentially be absent in a mouse or transwell model. Temperature has been known to have an effect on the gut microbiome and its' microbial composition, but little is known in terms of how to prevent or manipulate this alteration and whether the negatives can be lessened, or if the manipulation can provide some benefit to the host. The organ-on-a-chip can be used as a non-invasive way to study the human gut microbiome and epithelial cells *in vitro*, while still being physiologically relevant and minimizing the ethical concerns that could be present in human studies.

This study aims to collect preliminary data to determine if gene expression in gut epithelial cells is influenced by the presence of a fecal sample at hypoxic, hyperthermic conditions. We hypothesize that, upon the introduction of a fecal treatment, human epithelial cells will show expression consistent with human gut cells *in vivo*, and that this method could be used to study temperature effects in future studies.

## **Methods**

### Organ on a chip system

The experiment was performed using the Emulate Colon Intestine-Chip Culture protocol (Emulate, USA). Human Microvascular Endothelial Cells (HMVECs), HT-29 colonic cells, and Caco-2 cells used were purchased from the ATCC. The HT-29 and Caco-2 cells are both derived from human colon adenocarcinomas, and are commonly used in gut tissue studies. 36 chips were prepared at the same time. Chip packaging was sprayed and put into the biosafety cabinet, and chips were placed into a square cell culture dish, 6 per dish. An empty 15 mL conical tube was wrapped with foil for preparation of the ER-1 solution, which is light sensitive and is used to activate the surface of the chip's extracellular matrix attachment. The biosafety cabinet lights were turned off, and 9 mL of ER-2 solution was pipetted into the conical tube. 1 mL of ER-2 was pipetted into the ER-1 powder vial, and the vial was capped, inverted to collect any powder on the rim, and 1 mL of the vial contents were transferred to the conical tube. Using a P200 and 200  $\mu$ L filtered tips, 200  $\mu$ L of the ER-1 solution was drawn up. 20  $\mu$ L of the solution was added to the bottom channel inlet, until a small pool was formed at the outlet. Without releasing the plunger, 50  $\mu$ L was added to the top channel inlet, again until a pool formed at the outlet. Any excess ER-1 solution on the surface was aspirated using the pipettor. 200  $\mu$ L should be enough solution for 3 chips at a time. This was repeated for all 36 chips. If bubbles were present in either channel, the channels were washed with ER-1 to remove them, or, if needed, the channels can be aspirated, and new ER-1 solution can be re-added slowly. When no bubbles are present, the chips were put into a UV lightbox, one dish per box at a time, and the chips were activated under UV light for 15 minutes. When the UV activation is done, the chips were brought back into the biosafety cabinet, and ER-1

solution was aspirated from both channels. Each channel is then washed with 200  $\mu$ L of ER-2 solution, aspirated, and then washed with 200  $\mu$ L of PBS twice, with PBS left in the channel after the second wash until the extracellular matrix (ECM) is ready. During the UV activation, the ECM can be prepared. One aliquot of fibronectin (1 mg/mL), Collagen IV (1 mg/mL), and Matrigel was thawed on ice. 5 mL of ECM was made, as the total volume needed is given as 1.5 mL per 12 chips, and 36 chips requires 4.5 mL of ECM with the extra 500  $\mu$ L for errors in coating. 1000  $\mu$ L of Collagen IV, 150  $\mu$ L of fibronectin, and 3850  $\mu$ L of Matrigel were combined in a 15 mL conical tube. Final working concentration of each was 200  $\mu$ g/mL Collagen IV, 30 $\mu$ g/mL fibronectin, and 770  $\mu$ g/mL Matrigel. ECM solution was kept on ice until ready to use. The PBS in the channels were then aspirated, and 200  $\mu$ L pipette tips were loosely added to the outlets of both channels. 100  $\mu$ L of ECM was drawn up using a P200, and 50  $\mu$ L of ECM was added to each channel. The ECM was pushed through until the liquid equalizes in the inlet and outlet pipette tip, and the tip was ejected from the pipettor with the tip still inserted into the inlet channel. This was repeated for each chip, and each chip was checked for bubbles. Some bubbles were present, so the ECM was pipetted up and down to dislodge bubbles, and in some cases, aspirated and reintroduced slowly. When no bubbles were present, the chips were stored in a deli fridge at 4°C until they were ready to be seeded (3 days).

HMVEC cells were harvested by aspirating culture media and adding 10 mL of PBS to wash the surface of the flask. The PBS was aspirated, and 5 mL Trypsin was added, enough to cover the bottom of the flask. The flask was incubated at 37C for about 5

minutes, and then taken out and tapped to ensure detachment. 5 mL of warmed HMVEC media was added to the flask, and the contents of the flask were transferred to a 15 mL conical tube. The conical was then centrifuged at 300 rcf for 5 minutes, the supernatant was removed, and the pellet was resuspended with 1 mL of warmed HMVEC media. 10  $\mu$ L of the cell suspension was added to a 1.5 mL tube, along with 10  $\mu$ L of trypan blue. 10  $\mu$ L of this solution was inserted into a hemocytometer, and cells were counted under a microscope. 740  $\mu$ L of the cells were then mixed in a separate tube with 1260  $\mu$ L of the warmed HMVEC media to make a cell density of  $10 * 10^6$  cells/mL. The bottom channel media was then aspirated, and 30  $\mu$ L of HMVEC cells were pushed in until the liquids equalized in the inlet and outlet tips. The first chip seeded was checked under a microscope to ensure the correct density was seeded. This was repeated for all 36 chips, working with 3 chips at a time. The chips were then inverted on a test tube rack for about an hour to allow for attachment, before being flipped back upright for top channel seeding. Caco2 and HT29 were harvested mixed in a 3:1 ratio using the same methods described for the HMVEC cells using warmed Caco2 media, and seeded into the top channel at a density of  $3.75 * 10^6$  with the same seeding method as HMVEC cells, but with 35  $\mu$ L added to the top channel and without the 1-hour inversion. When the top channel has been seeded, the chips are incubated overnight at 37C.

HMVEC and Caco2 media were equilibrated using a Steriflip unit the next day. Warmed Caco2 and HMVEC media were added to 3 50-mL conical tubes per media, making 150 mL of each media. The Steriflip unit was then attached to the conical, which was hooked up to a vacuum, inverted and was degassed for 6 minutes. This was repeated for each

conical until all 6 were degassed. To prime the pods, the pods and accompanying trays were sanitized before being put into the BSC, and the pods were put into the trays. 4 mL of the equilibrated HMVEC and Caco2 media was put into the bottom and top channel inlets of the pods respectively, and a small amount was pipetted onto each outlet port. The pods were then put into the Zoe, where a priming cycle was run by selecting “Prime” and pressing start. Each pod was checked to ensure priming, in which 4 droplets are present on the underside of the pod. While this occurred, the pipette tips were removed from the chips, and ~100  $\mu$ L of the respective medias pushed through each channel twice, with any excess being aspirated from the surface, and small droplets were placed on each port. This was repeated for all chips. To dock the chips, each chip was slid into the tracks on the underside of each pod, and the tab was depressed in and up into the chip, taking care to be firm enough to be able to lock it in, but gentle enough to ensure that it locked without a snapping noise being made. The pods were then placed into the trays, 6 pods per tray, and the trays were then put back in the Zoe. Flow rate was set to 30  $\mu$ L/hr for both channels, and the chips were then set to the “Regulate” setting. The regulate cycle lasts for about 2 hours, and when completed, the Zoe will then run at the preset parameters. Pods were checked every other day, and 4 mL of media was replaced in the pods as needed for the next 12 days. Stretch was initiated at 5%, 0.15 Hz on the 4<sup>th</sup> day of this period by pausing the Zoe, setting the parameters, and then reactivating the Zoe, which was increased to 10% stretch, 0.2 Hz on Day 8.

#### Final experimental preparations

On Day 8, a fecal slurry was diluted 2-fold and split into 500  $\mu\text{L}$  aliquots in the H35 hypoxystation. On Day 11, the pods were paused, and the top channel media was replaced with 4 mL of sterilized “Gut Juice” (which consisted of HBSS, essential and non-essential amino acids, Glutamax, HEPES, sodium bicarbonate, L-arabinose, mucin, hemin, and vitamin K), as well as 2  $\mu\text{L}/\text{mL}$  of FITC-Dextran. The chips were separated and labelled into 6 treatment groups of 6 chips. Each treatment group had 3 “no-treats” which included 10  $\mu\text{L}/\text{mL}$  of Penicillin-Streptomycin antibiotic in the gut inlets and acted as within-group controls, and 3 “full fecal” which included chips dosed with the fecal slurry. They were then further divided into temperature groups, with 12 chips at 30°C, 37°C, and 42°C, with 6 chips at anaerobic levels and 6 at aerobic levels. Due to constraints on the number of Zoe’s available, this experiment was split into 2 “rounds” with round 1 containing 30°C and 37° aerobic and 30°C and 42°C hypoxic conditions and round 2 containing 42°C aerobic and 37°C hypoxic conditions.

### Dosing and Collections

Before dosing, gut and vascular compartment effluent was collected into 1.5 mL tubes for the 0-hour timepoint. Gut compartments of the chips were dosed with 25  $\mu\text{L}$  of warmed fecal slurry and chips were allowed to rest in the Zoe for one hour to acclimate before being set to flow for 120  $\mu\text{L}/\text{hr}$  for 3 hours. At time points 4- and 8-hours, effluent from both channels was collected into separate tubes, vascular effluent was spun down, and supernatant was collected into another tube. Tubes were then frozen at -80°C. At time points 12-, 24-, and 48- hours, an additional flush of 800  $\mu\text{L}/\text{hr}$  was performed for 5 minutes before sampling occurred. After the 48-hour collection, chips were lysed using

trypsin in the bottom channel and Ripa Buffer in the top channel and transferred to tubes, both were spun down, and supernatant was removed. RNA extraction was done using the ThermoFisher *mirVana* PARIS kit (ThermoFisher, USA).



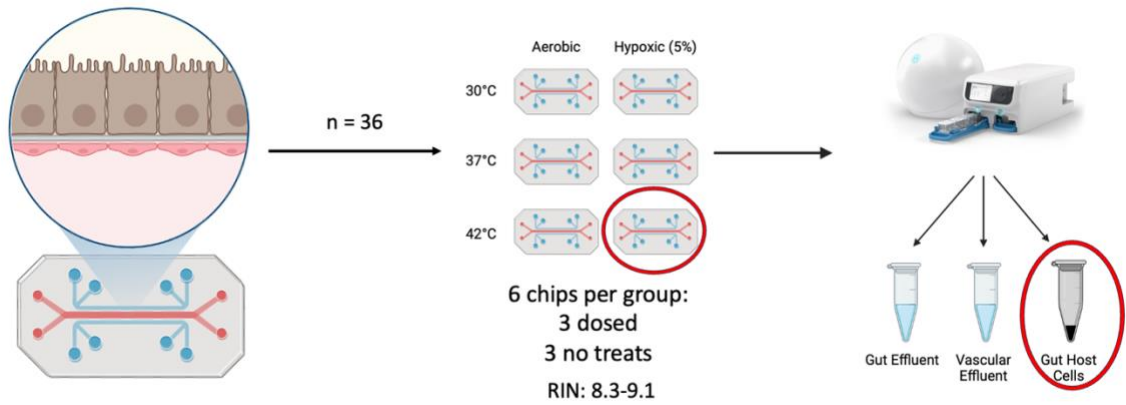


**Figure 1.** Graphical representation of the experimental workflow for the organ-on-a-chip. 36 chips were seeded and separated into 6 groups of 6 chips based on oxygen level and temperature. For the purposes of this paper, only the gut host cells of the 42°C hypoxic group were sequenced (Red Circles). Created with BioRender.com.

### Library Preparation

RNA Host samples were PolyA enriched and prepared using the Illumina Stranded mRNA Prep, Ligation Kit (Illumina, USA). Before preparing, each RNA host sample was diluted in a 1:10 ratio (5  $\mu$ L of sample:45  $\mu$ L of nuclease free water), and RNA concentrations were collected using a Qubit fluorometer and RNA Integrity Number (RIN) values were collected using Agilent TapeStation. Sample 6 read too high on the fluorometer, and as it was diluted down at a 1:10 ratio, the concentration was assumed to be 10 times higher than that read on the fluorometer. The first 7 host samples were prepped together, along with a negative control that comprised of nuclease-free water. Approximately 200 ng of the diluted sample was transferred to strip tubes and numbered 1-7, with a negative control numbered as 8, and were diluted to a volume of 25  $\mu$ L with nuclease free water. 25  $\mu$ L of RPBX was added to each tube, pipetted 10 times to mix, and then the mRNA\_CAP program (65°C for 5 minutes, 4°C for 30 seconds, 23°C for 5 minutes and hold at 23°C) was run on a thermal cycler. The strip tubes were then centrifuged at 280 x g for 10 seconds, and then placed on a magnet for 2 minutes. Supernatant was removed, the strip tubes are removed from the magnet and 100  $\mu$ L of bead washing buffer was added to each well and mixed with a pipette. The strip tubes were placed back on the magnet for 2 minutes, supernatant was removed, the tubes were taken off magnet, and 25  $\mu$ L of elution buffer was added and mixed by pipette to resuspend the beads. The strip tubes were then centrifuged at 280 x g for 10 seconds, and the mRNA\_ELT (80°C for 2 minutes, hold at 25°C) program was run on the thermal cycler. While this is running, the fragmentation master mix was made by adding 10.5  $\mu$ L each of EPH3 and nuclease free water per sample. The strip tubes were centrifuged at 280

x g for 10 seconds, and 25  $\mu$ L of bead beating buffer was added and mixed in each tube. The strip tubes were allowed to incubate at room temperature for 5 minutes, before being put on magnet for 2 minutes. 50  $\mu$ L of supernatant was removed, before being taken off magnet and 100  $\mu$ L of bead washing buffer was added and mixed by pipette. The tubes were put back on magnet for 2 minutes, supernatant was discarded, removed from the magnet, and 19  $\mu$ L of the fragmentation master mix was added to each tube and pipetted to resuspend the beads. The tubes were allowed to incubate at room temp for 2 minutes, centrifuged at 280 x g for 10 seconds, and the DEN94\_8 program (94°C for 8 minutes, 4°C hold) was run on the thermal cycler. The tubes were centrifuged at 280 x g for 10 seconds, placed on magnet for 2 minutes, and then 17  $\mu$ L of supernatant was transferred to a new set of numbered strip tubes. The old strip tubes can be discarded.

The first strand synthesis master mix is made by combining 9  $\mu$ L of FSA and 1  $\mu$ L of reverse transcriptase per sample, and 8  $\mu$ L was added to each tube and mixed by pipetting 10 times. The FSS program (25°C for 10 minutes, 42°C for 15 minutes, 70°C for 15 minutes, 4°C hold) was then run on the thermal cycler. When finished, the tubes were centrifuged at 280 x g for 10 seconds, 25  $\mu$ L of SMM was added to each tube, and the Second Strand Synthesis program (16°C for 60 minutes, 4°C hold) was run on the thermal cycler. When finished, the tubes were centrifuged at 280 x g for 10 seconds, and 90  $\mu$ L of AMPure XP is added to each tube and mixed by pipette to resuspend the beads. The tubes incubate at room temperature for 5 minutes, were placed on magnet for 5 minutes, and 130  $\mu$ L of supernatant was removed. The beads are then washed twice by adding 175  $\mu$ L of fresh 80% EtOH, waiting 30 seconds, and then removing the

supernatant. The tubes then air dry on the magnet for 2 minutes, are removed from the magnet, and 19  $\mu\text{L}$  of resuspension buffer was added to each tube and mixed by pipette. The tubes are then centrifuged at 280 x g for 10 seconds, put on magnet for 2 minutes, and then 17.5  $\mu\text{L}$  of supernatant is transferred to a new set of numbered strip tubes. The old strip tubes were discarded at this time.

12.5  $\mu\text{L}$  of ATL4 is added to each tube, pipetted 10 times to mix, and then the ATAIL program (37°C for 30 minutes, 70°C for 5 minutes, 4°C hold) was run on the thermal cycler. The tubes are then centrifuged at 280 x g for 10 seconds, and 5  $\mu\text{L}$  of RNA index anchors and 2.5  $\mu\text{L}$  of LIGX were added to the tubes in that order, and pipetted 10 times to mix. The LIG program (30°C for 10 minutes, 4°C hold) is then run on the thermal cycler. When finished, the tubes were centrifuged at 280 x g for 10 seconds, and 5  $\mu\text{L}$  of STL was added and mixed by pipetting to stop ligation. 34  $\mu\text{L}$  of AMPure XP was added to each tube, incubated at room temperature for 5 minutes, placed on magnet for 5 minutes, and 67  $\mu\text{L}$  of supernatant was removed. The beads are again washed twice as previously described, air dried on the magnet for 2 minutes, and 22  $\mu\text{L}$  of resuspension buffer was added to each tube and mixed by pipetting to resuspend the beads. The tubes are incubated at room temperature for 2 minutes, centrifuged at 280 x g for 10 seconds, placed on magnet for 2 minutes, and 20  $\mu\text{L}$  of supernatant was transferred to a new set of numbered strip tubes. The old strip tubes were then discarded.

Using a new pipette for each index, 10  $\mu\text{L}$  of UD indexes (Set B in this case) were transferred from the index adapter plate to the strip tubes, and then 20  $\mu\text{L}$  of EPM was

added to each tube and pipetted 10 times to mix. The PCR program was then run on the thermal cycler with 12 PCR cycles for 200 ng of input amount (98°C for 30 seconds, 12 cycles of 98°C, 60°C and 72°C for 10, 30, and 30 seconds respectively, 72°C for 5 minutes and a 4°C hold). When finished, the tubes were centrifuged at 280 x g for 10 seconds, and 50 µL of AMPure XP was added to each tube and mixed. The tubes were then incubated at room temperature for 5 minutes, put on magnet for 5 minutes, and 90 µL of supernatant was discarded. The beads are again washed twice as previously described, air dried on the magnet for 2 minutes, and 17 µL of resuspension buffer is added to each tube and mixed by pipetting to resuspend the beads. The tubes are incubated at room temperature for 2 minutes, centrifuged at 280 x g for 10 seconds, placed on magnet for 2 minutes, and 15 µL of supernatant was transferred to a final new set of numbered strip tubes. The old strip tubes were then discarded.

Throughout this protocol, there are several safe stopping points where the tubes can be frozen and stored at -25 to -10. However, it is recommended to go through the protocol all at once to prevent degradation of the sample. 2 µL of each sample are used to quantify library concentration using the Qubit fluorometer, and another 2 µL are used to check library quality using the TapeStation.

### Sequencing

To remove the adapter dimer, a left-side cleanup was performed by adding AmpureXP beads equal to 0.8 times the sample volume. The samples are then centrifuged, vortexed, and centrifuged again, and then sat for 5 minutes. The samples were then put on magnet

for 2 minutes, supernatant was removed, and the beads were washed once with 100  $\mu$ L of 80% ethanol. After 30 seconds, the ethanol was removed, air dried for 2 minutes, and 14  $\mu$ L of resuspension buffer was added. Finally, 2  $\mu$ L of each sample are used to quantify library concentration, and another 2  $\mu$ L are used to check library quality as described previously.

Samples were put into a script to normalize to 2 nM concentration, and gave a dilution factor and amount to pool for each sample. Samples were also set to target 22.75 million reads each. An Illumina NextSeq 1000/2000 P1 Reagent Cartridge (Illumina, USA) was pulled from the freezer and left to thaw on the lab bench for 8 hours. After ~8 hours, the cartridge was then put into the fridge until use. As the script gave a dilution factor of 1, samples were not diluted, and were pooled with nuclease-free water for a total volume of 250  $\mu$ L. 8  $\mu$ L of the pooled library and 16  $\mu$ L of RSB w/ Tween were vortexed, centrifuged, and concentration was quantified on Qubit. The cartridge was taken out, inverted 10 times each way (10 with the left hand on top, 10 with the right hand on top), and 23.2  $\mu$ L of the library was loaded into the cartridge. The cartridge was loaded into the Illumina NextSeq 1000/2000 sequencer, and left to run until completion. When completed, the resulting sequences were then moved into the Ohio Supercomputer for data analysis.

### Statistical Analysis

Sample 7 (42O2NT 1) was omitted from data analysis, as it was not in the 42 Hy treatment group, and its' replicates were not prepped alongside it. Raw data was

produced using the Ohio Supercomputer (OSC), and analyzed using RStudio. Adapters and low-quality bases were trimmed using Trimmomatic, and fastqc was used to generate a quality control report. The Spliced Transcripts Alignment to a Reference (STAR) v2.7.11b was used to align the reads to the GRCh38.p14 Human Reference Genome (NCBI). MarkDuplicates was used to identify duplicate reads, and featureCounts was used to map reads to the genomic features in the human genome to produce the raw data. This raw data was then put into RStudio, and DESeq2 was used to normalize (by way of the median of ratios method) and perform a Wald test on the data to generate adjusted p-values. Anything significant was identified as having at least a log2FoldChange of 2 or greater and p-value of less than 0.01. A volcano plot was then generated in RStudio to represent the final data.

## **Results**

### Pre-Library Prep Concentrations and Integrity

We selected 6 samples for analysis that included the 42°C Hypoxic treatment, as it would give comparison within a single group. Samples were quantified at a concentration between 29.5 ng/μL to 144 ng/μL (Table 1). Each sample was assigned an RNA Integrity Number (RIN) on the TapeStation as a method for quality control, with 1 being severely degraded and 10 being a perfect sample with no degradation at all. Scores for the 6 samples ranged from 8.3-9.1 (Table 1), which are viable for a PolyA enrichment protocol (which normally calls for RIN above 7-8).

<b>Sample Name</b>	<b>Sample Number</b>	<b>Concentration (ng/<math>\mu</math>L)</b>	<b>1:10 Dilution Concentration (ng/<math>\mu</math>L)</b>	<b>RIN</b>
42 HY NT Gut 1	1	95	N/A	9
42 HY NT Gut 2	2	29.5	N/A	8.6
42 HY NT Gut 3	3	37.9	N/A	8.3
42 HY FF Gut 1	4	49.7	N/A	8.7
42 HY FF Gut 2	5	67	N/A	8.9
42 HY FF Gut 3	6	N/A	11.1	9.1

**Table 1.** Pre-library prep concentrations are listed in ng/ $\mu$ L, as well as RNA Integrity

Numbers (RINs). Sample 6 had to be diluted, as the undiluted concentration was too high for the Qubit fluorometer to read.



### Post-Library Prep

Concentrations of the samples after being prepared ranged from 0.940 ng/ $\mu$ L and 2.64 ng/ $\mu$ L, with the negative control quantified at 0.560 ng/ $\mu$ L (Table 2). After the left-side cleanup was performed, concentrations of the samples ranged from 0.057 ng/ $\mu$ L to 1.05 ng/ $\mu$ L, with the negative control reading at 0.198 ng/ $\mu$ L (Table 2). This was lower than the desired range of 4-5 ng/ $\mu$ L minimum for each sample, and one concentration being lower than the negative control also raised some concerns. TapeStation average peak size ranged from 300-450, which is within the expected range for paired-end sequencing of 2x150 base pairs (Table 2, Figure 2). Samples 1 and 2 had three peaks that were distorted and unlike the other TapeStation graphs, and so sizing peaks were estimated based on the center peak (Figure 2). The final pooled library concentration was 1.26 ng/ $\mu$ L, which is sufficient to support sequencing (>0.70 ng/ $\mu$ L).

<b>Sample #</b>	<b>Sample Name</b>	<b>Concentration (ng/μL)</b>	<b>Concentration post cleanup (ng/μL)</b>	<b>Avg Size (bp)</b>
1	42 Hy NT	0.967	0.41	400
2	42 Hy NT	1.53	0.516	400
3	42 Hy NT	1.63	0.182	400-450
4	42 Hy FF	2.64	1.05	375
5	42 Hy FF	0.94	0.495	300
6	42 Hy FF	2.26	0.057	325
NCL		0.56	0.198	350

**Table 2.** Post-library prep concentrations are listed in the third column in ng/μL.

Concentrations of the prepped samples after the left side cleanup are in the fourth column, and the size of the library (in units of base pairs) taken from the TapeStation are in the last column.

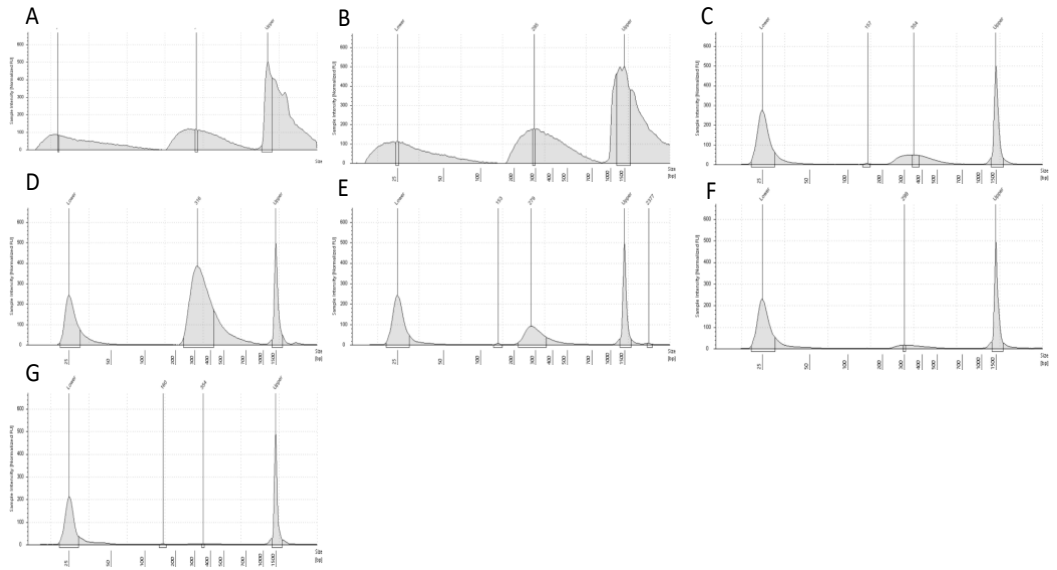


**Figure 2.** (A-G) TapeStation electrophoresis graphs of samples 1-6 and the negative control. An average bp size was estimated based on peaks and where the middle curve started and ended. (A, B) For samples 1 and 2, due to the odd shape of the curve, an average bp size of 400 was estimated for both.

### Effects of Fecal Treatment on Hypoxic Host Sample Gene Expression

We found that 21,686 total genes were mapped to the genomes of these 6 samples; however, only 43% (9493/21686) of these genes were assigned a p-value, indicating that 57% of genes were either considered outliers or had too low of mean normalized read counts mapped to the genome, which could indicate that an important gene could have been left out of the analysis. There were 66 genes that had a p-value of less than 0.01, indicating that these genes had a significantly high chance of being upregulated or downregulated when exposed to a fecal treatment (Table 3). These genes could be sorted into four categories based on their general function, which included roles in the immune response, host metabolism (such as lipid absorption), cellular growth, structure, and differentiation, and if it was involved in enzymatic processes. The majority of these 66 genes were classified as “Immune Response” genes (28/66), which is consistent with our hypothesis as the introduction of a fecal sample will introduce bacteria to the tissue, and the tissue would need to defend itself against any potentially harmful microbes in the introduced sample. Based on the significance threshold of  $p < 0.01$  and a  $\log_2\text{FoldChange}$  of  $|\geq 2|$ , only 5 genes were shown to be significantly upregulated (Table 3). These 5 genes were the HES1 gene (which had a  $\log_2\text{FoldChange}$  of  $\sim 2.06 \pm 0.148$  and had the lowest p-value of the all genes at  $2.50 * 10^{-40}$ ), the RHOV gene (which had a  $\log_2\text{FoldChange}$  of  $\sim 3.35 \pm 0.31$  and p-value of  $9.93 * 10^{-24}$ ), the IL6 gene (which had a  $\log_2\text{FoldChange}$  of  $\sim 2.47 \pm 0.27$  and a p-value of  $4.79 * 10^{-17}$ ), the APOA4 gene (which had a  $\log_2\text{FoldChange}$  of  $\sim 2.96 \pm 0.50$  and a p-value of  $1.38 * 10^{-6}$ ), and the CXCL1 gene (which had a  $\log_2\text{FoldChange}$  of  $\sim 2.23 \pm 0.38$  and a p-value of  $41.50 * 10^{-6}$ ). No genes that reached both significance thresholds had a negative  $\log_2\text{FoldChange}$ , indicating that

no genes were significantly downregulated, although some genes like the RNR2 gene (involved in deoxyribonucleotide biosynthesis) experienced some level of downregulation, but did not have a high enough log<sub>2</sub>FoldChange to be considered significant (Table 3, Figure 3). We also did not see any presence of heat shock proteins, although this could be due to a later time point collection, and we might see the presence of these proteins had we taken a timepoint closer to inoculation.

gene_id	Average Reads	log2FoldChange	log2FoldChange Standard Error	padj	Up or down regulated
<b><u>Immune Responses</u></b>					
HES1	587	2.06	0.148	2.50E-40	Up
NR4A1	645	1.79	0.147	1.60E-30	Up
IL6	122	2.47	0.267	4.79E-17	Up
ZFP36	654	1.26	0.147	1.84E-14	Up
CXCL8	160	1.61	0.222	5.07E-10	Up
ELF3	1300	0.81	0.118	8.10E-09	Up
NCOA7	274	1.22	0.18	1.07E-08	Up
TNFAIP2	551	1.08	0.174	3.13E-07	Up
SOCS3	215	1.25	0.202	3.49E-07	Up
NFKBIA	481	0.89	0.145	4.86E-07	Up
RNR2	6740	-0.73	0.122	1.31E-06	Down
CXCL1	55.8	2.23	0.376	1.50E-06	Up
ATF3	664	0.88	0.153	3.96E-06	Up
FGA	113	1.61	0.314	9.52E-05	Up
AGT	188	1.17	0.241	0.000300	Up
BCL3	295	0.84	0.175	0.000456	Up
TXNIP	674	0.87	0.186	0.000709	Up
CEBPD	239	0.86	0.185	0.000735	Up
SOD2	1060	0.78	0.17	0.000949	Up
PDZK1IP1	73.4	1.37	0.309	0.00197	Up
SDC4	646	0.61	0.139	0.00201	Up
FGG	67.6	1.5	0.344	0.00265	Up
LIF	269	0.73	0.174	0.00473	Up
TTYH3	182	0.9	0.214	0.00509	Up
MUC5B	35.8	1.89	0.453	0.00565	Up
ETS2	512	0.6	0.146	0.00604	Up
BNIP5	118	1.16	0.282	0.00674	Up
ZNF292	189	-0.81	0.198	0.00702	Down
<b><u>Host Metabolism</u></b>					
APOA4	39.1	2.96	0.497	1.38E-06	Up
CLDN4	2090	0.59	0.121	0.000264	Up
CDC42EP2	315	0.85	0.174	0.000300	Up
FABP1	98	1.36	0.29	0.000579	Up
LYPD2	53	1.5	0.364	0.006220	Up
<b><u>Cellular Growth and Structure</u></b>					

RHOV	102	3.35	0.31	9.93E-24	Up
BHLHE40	793	1.13	0.13	5.54E-15	Up
FOSB	252	1.45	0.188	1.72E-11	Up
VWA1	513	1.06	0.167	1.54E-07	Up
SOX9	515	1.07	0.173	3.49E-07	Up
ID1	318	1.05	0.176	1.17E-06	Up
EGR1	1400	0.83	0.14	1.53E-06	Up
S100A9	394	1.09	0.195	9.61E-06	Up
FOS	697	0.73	0.142	0.000102	Up
PLK2	614	0.97	0.192	0.000143	Up
BTG2	151	1.26	0.251	0.000173	Up
MYBL2	150	1.39	0.281	0.000241	Up
KLF10	357	0.97	0.205	0.000529	Up
S100A8	82.4	1.35	0.305	0.00201	Up
DDX3X	1002	-0.45	0.116	0.00318	Down
CSF2	68.3	1.82	0.446	0.00713	Up
JUNB	987	0.64	0.158	0.00818	Up
HBEGF	420	0.73	0.18	0.00869	Up
CHRD	124	1.15	0.287	0.00900	Up
<b><u>Enzymatic Activity</u></b>					
ALPP	404	1.14	0.162	2.01E-09	Up
B3GNT7	181	1.24	0.225	1.41E-05	Up
TRIB1	924	0.88	0.168	7.14E-05	Up
DUSP5	1700	0.59	0.121	0.000249	Up
UBE2S	723	0.66	0.136	0.000316	Up
SERPINA1	403	0.81	0.168	0.000366	Up
SERPINB9	73.9	1.66	0.344	0.000377	Up
NNMT	381	0.86	0.18	0.000485	Up
SERPINA1_1	327	0.79	0.18	0.00201	Up
TXNRD1	1580	-0.47	0.114	0.00573	Down
RESF1	287	-0.72	0.176	0.00626	Down
PTGES	248	0.79	0.194	0.00715	Up
PLAU	641	1.47	0.367	0.00874	Up
CKB	450	0.59	0.148	0.00874	Up

**Table 3.** DESeq2 table showing up- or downregulation when a fecal sample is introduced

to the chip. All 66 genes with a significance of  $p < 0.01$  are listed, separated by general gene function and sorted by adjusted p-value. Adjusted p-values were generated in the

DESeq2 program using the Wald test. Genes highlighted in yellow are considered to be significant based on the parameters set ( $p\text{-value} < 0.01$ ,  $\log_2\text{FoldChange} > 2.00$ ).

Standard errors in  $\log_2\text{FoldChange}$  are also listed. All values in the table have been rounded to 3 significant figures.



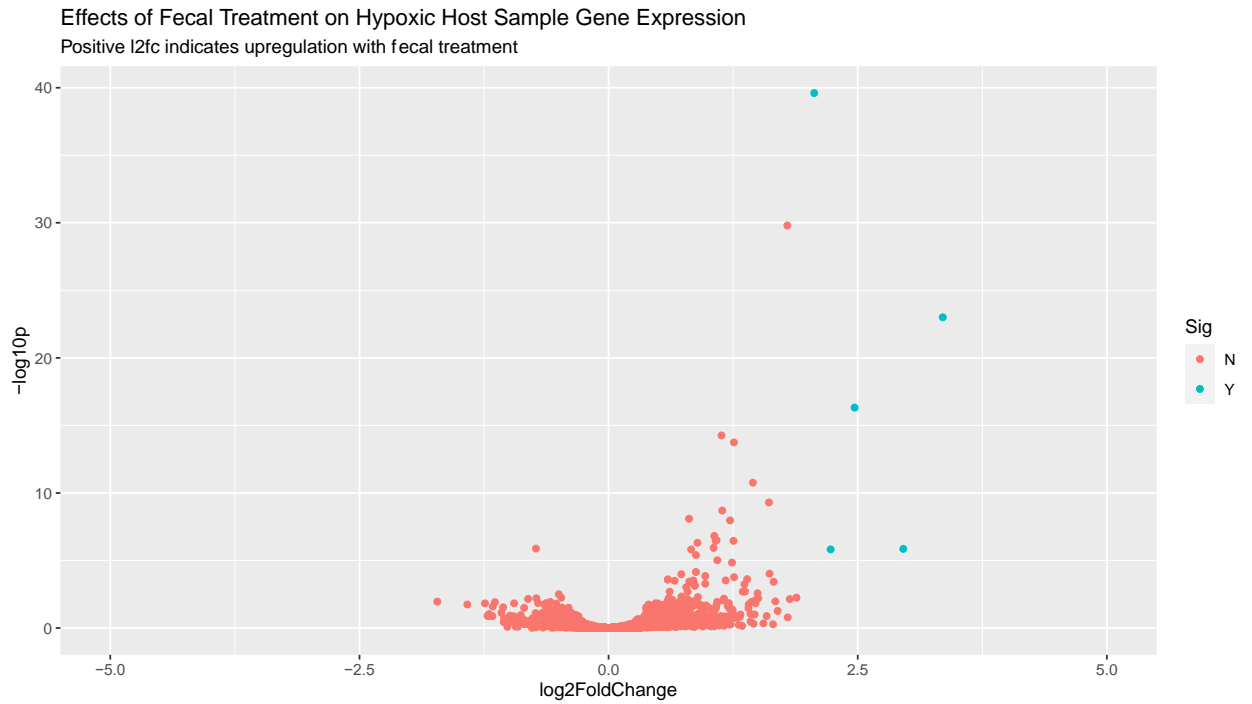


**Figure 3.** Volcano plot showing effects of fecal treatment on hypoxic host sample gene expression. Log2FoldChange is plotted on the X-axis vs. p-value on the Y axis. Each dot represents a single gene in the human genome, and a positive log2FoldChange indicates upregulation when exposed to the fecal sample vs no fecal treatment. Blue dots represent significant up/downregulation, indicating an adjusted p-value  $< 0.01$  and a log2FoldChange  $> 2.00$ , and red dots indicate no significance.

## Discussion

The goal of this study was to collect preliminary data to determine if gene expression in gut epithelial cells is influenced by the presence of a fecal sample at hypoxic, hyperthermic conditions. This study found that when the human gut epithelial cells are exposed to a fecal sample taken from a human donor, the host epithelial cells experience mostly upregulation of genes (mainly involving the immune response), along with a non-significant trend toward limited downregulation of other genes. These findings support our hypothesis that human epithelial cells *in vitro* show expression consistent with human gut cells *in vivo*, and that this method could be used to study temperature effects in future studies.

Significantly upregulated epithelial cell genes could be categorized into four generalized functions involving immune response, host metabolism, cellular growth and structure, and other enzymatic activity, with immune response genes being the most abundant out of the 4 groups. These genes would be critical in defending the cell tissue against harmful bacteria that could be present when the fecal sample is introduced. The 5 genes that were significantly upregulated based on our cutoffs were the HES1, IL6, CXCL1, RHOV, and APOA4 genes. The HES1 (hes family bHLH transcription factor 1) gene is involved in prevention of gut dysbiosis, where mouse studies have shown that a HES1 deletion leads to a higher susceptibility to pathogenic bacteria colonization in the gut, as well as an increase in gut inflammation (Guo et al. 2018). This is consistent with our results, as an upregulation in HES1 would indicate that the host cells are preventing pathogen

colonization when fecal samples are introduced. The IL-6 (interleukin 6) gene is produced in response to infection and injury to tissues, and can be released by endothelial cells to stimulate acute phase responses to defend the host during inflammation, which is consistent with our results as IL-6 is upregulated to defend the host from harmful bacteria in the fecal sample (Tanaka, Narazaki, and Kishimoto 2014). The CXCL1 (chemokine ligand 1) gene is a neutrophil chemoattractant that can recruit neutrophils to defend the host from bacterial infection, which is consistent with our results in that the introduction of bacteria would cause the host cells to produce this chemoattractant to defend against the potentially pathogenic bacteria in the gut (De Filippo et al. 2013). The RHOV (Ras Homolog Family Member V) gene is a GTPase that is predicted to be involved in Cdc42 protein signaling transduction and endocytosis, but is understudied (NIH). However, other Rho GTPases have been known to be involved in actin cytoskeleton reorganization and tissue structure, which coincides with our results in that upregulation would indicate that the host tissue is altered due to the introduction of bacteria, and that the Rho gene is needed to protect tissue homeostasis (Pradhan et al. 2021). The ApoA4 (Apolipoprotein A-IV) protein is involved in the activation of the lecithin:cholesterol acyltransferase, which is involved in the reverse cholesterol transport pathway that transfers excess cholesterol to the liver for excretion, as well as lipid metabolism (Steinmetz and Utermann 1985, Rousset et al. 2013, Wang et al. 2015). The ApoA4 upregulation makes sense in the context of our results, as when gut bacteria produce fatty acids such as butyrate, acetate, and propionate, the host needs to account for the increase, and so produces more ApoA4 for lipid metabolism (Qu et al. 2019, He et al. 2020). Further

studies would be needed to characterize what metabolites are being produced, and to the extent of how this upregulation effects lipid metabolism.

The functional category of enzymatic activity did not have any significant genes being upregulated or downregulated, but still hit the significance threshold. Despite this, some of the significantly upregulated genes had multiple functions that could fit into the other categories, such as the RHOV gene dealing with immune response (Pradhan et al. 2021). Overall, the results of most host epithelial genes being upregulated, and the genes being significantly upregulated being characterized as generally “immune response” genes, makes sense in the context of this study, as the host tissue would need to upregulate the genes that are required to protect and defend the host from invasion of potentially dangerous bacteria that could harm the host.

Due to time constraints, and the absence of a previous library prep pipeline established in the laboratory or in literature, this study only evaluated the effect of temperature on the chips that were treated in a hypoxic setting at 42°C. As the average normal human core temperature is generally accepted to be 37°C, further studies will need to be done to determine the effectiveness of using the organ-on-a-chip system on samples treated at normal temperature like 37°C or colder temperatures such as the 30°C treatment group that was included in the original chip experiment group. Also, due to the small sample size in this study (6 samples in a single treatment group), it is possible that the log2FoldChange threshold of  $|2|$  would be too strict, and could potentially exclude genes that are significantly up or downregulated when this pipeline is run on a larger dataset

that includes more samples. To counteract this, a looser threshold of  $|1.5|$  might be recommended, depending on how many significant genes this gives. The final library concentration values were somewhat lower than what we were expecting, especially given the high starting RNA concentration, indicating a potential loss in RNA either during the actual library prep protocol or the length of time between initial quantification and prep. The library prep protocol will need to be further optimized to lessen the loss of RNA over the course of the pipeline, although the current pipeline gave enough reads to allow for sufficient analysis for proof of concept.

As mentioned above, further studies are required to determine whether there are any significantly upregulated or downregulated genes in the other treatment groups and between each treatment group in this study. Currently, the next course of action is to further optimize the library preparation protocol, and then sequence the host endothelial samples from the other treatment groups, and assess the alpha and beta diversities of gene regulation in those groups. Further studies are also necessary to determine if there are any shifts in the gut microbiome due to temperature, and see if there is a specific temperature or range of temperatures where that shift can occur, and whether this contributes to changes seen in the gut epithelial tissue. In doing this, the gut-on-a-chip could be used to see if there is a way to counteract any negative shifts in the microbiome once it reaches the temperature that the shift occurs at, whether that be by the introduction of probiotics, or by studying temperature acclimation. Further studies could also be done using a whole-body chip system that could be built in the future. By linking the gut chip with something like a brain-on-a-chip system, the effects of temperature on the gut

microbiome could also potentially show a change in cognitive ability, and if the counteracting done on the gut shift could also provide beneficial or detrimental effects on other organs like the brain.

## **Conclusion**

The goal of this study was to collect preliminary data to determine if gene expression in gut epithelial cells is influenced by the presence of a fecal sample at hypoxic, hyperthermic conditions. We found that when the human host endothelial cells were exposed to a fecal treatment, there was significant upregulation of a majority of genes, with most of the upregulation being involved in immune system responses to the bacteria being introduced. However, some RNA was lost between initial quantification and the final library concentration, and around 57% of genes in the human genome had an insufficient number of reads mapped to them, so it is likely that the significance of gene upregulation or downregulation is being underrepresented. Further studies will need to be done to verify the effectiveness of this model at other temperatures, such as at 30°C or 37°C. Overall, this model is a new, more physiologically relevant way to study the effects of temperature on the gut microbiome, and can be used to study methods to counteract negative impacts associated with these temperature shifts.

Article is approved for Distribution A, public clearance, on 13 Feb 2024 under the originator reference number: RH-24-125354

### Chapter 3: References

- Aagaard, K., Ma, J., Antony, K. M., Ganu, R., Petrosino, J., & Versalovic, J. (2014). The placenta harbors a unique microbiome. *Science Translational Medicine*, 6(237).  
<https://doi.org/10.1126/scitranslmed.3008599>
- Armed Forces Health Surveillance Division. (2022, April 1). Heat illness, active component, U.S. Armed Forces, 2021. Military Health System.  
<https://www.health.mil/News/Articles/2022/04/01/Update-Ht-MSMR>
- Ashammakhi, N., Nasiri, R., Barros, N. R., Tebon, P., Thakor, J., Goudie, M., Shamloo, A., Martin, M. G., & Khademhosseini, A. (2020). Gut-on-a-chip: Current progress and future opportunities. *Biomaterials*, 255, 120196.  
<https://doi.org/10.1016/j.biomaterials.2020.120196>
- Bein, A., Shin, W., Jalili-Firoozinezhad, S., Park, M. H., Sontheimer-Phelps, A., Tovaglieri, A., Chalkiadaki, A., Kim, H. J., & Ingber, D. E. (2018). Microfluidic organ-on-a-chip models of human intestine. *Cellular and Molecular Gastroenterology and Hepatology*, 5(4), 659–668.  
<https://doi.org/10.1016/j.jcmgh.2017.12.010>
- Bettelheim, K. A., Breadon, A., Faiers, M. C., O'Farrell, S. M., & Shooter, R. A. (1974). The origin of O serotypes of Escherichia coli in babies after normal

delivery. *Journal of Hygiene*, 72(1), 67–70.

<https://doi.org/10.1017/s0022172400023226>

Bindels, L. B., Porporato, P., Dewulf, E. M., Verrax, J., Neyrinck, A. M., Martin, J. C., Scott, K. P., Buc Calderon, P., Feron, O., Muccioli, G. G., Sonveaux, P., Cani, P. D., & Delzenne, N. M. (2012). Gut microbiota-derived propionate reduces cancer cell proliferation in the liver. *British Journal of Cancer*, 107(8), 1337–1344.  
<https://doi.org/10.1038/bjc.2012.409>

Britton, R. A., & Young, V. B. (2014). Role of the intestinal microbiota in resistance to colonization by clostridium difficile. *Gastroenterology*, 146(6), 1547–1553.  
<https://doi.org/10.1053/j.gastro.2014.01.059>

Brugger, H., Durrer, B., Elsensohn, F., Paal, P., Strapazzon, G., Winterberger, E., Zafren, K., & Boyd, J. (2013). Resuscitation of avalanche victims: Evidence-based guidelines of the International Commission for mountain emergency medicine (ICAR MEDCOM). *Resuscitation*, 84(5), 539–546.  
<https://doi.org/10.1016/j.resuscitation.2012.10.020>

Bull MJ, Plummer NT. Part 1: The Human Gut Microbiome in Health and Disease. *Integr Med (Encinitas)*. 2014 Dec;13(6):17-22. PMID: 26770121; PMCID: PMC4566439.

Bäckhed, F., Ding, H., Wang, T., Hooper, L. V., Koh, G. Y., Nagy, A., Semenkovich, C. F., & Gordon, J. I. (2004). The gut microbiota as an environmental factor that regulates fat storage. *Proceedings of the National Academy of Sciences*, 101(44), 15718–15723. <https://doi.org/10.1073/pnas.0407076101>



Centers for Disease Control and Prevention. (2023, April 18). *Type 2 diabetes*. Centers for Disease Control and Prevention.

<https://www.cdc.gov/diabetes/basics/type2.html>

Chang, C., & Lin, H. (2016). Dysbiosis in gastrointestinal disorders. *Best Practice & Research Clinical Gastroenterology*, *30*(1), 3–15.

<https://doi.org/10.1016/j.bpg.2016.02.001>

Chevalier, C., Stojanović, O., Colin, D. J., Suarez-Zamorano, N., Tarallo, V., Veyrat-Durebex, C., Rigo, D., Fabbiano, S., Stevanović, A., Hagemann, S., Montet, X., Seimbille, Y., Zamboni, N., Hapfelmeier, S., & Trajkovski, M. (2015). Gut microbiota orchestrates energy homeostasis during cold. *Cell*, *163*(6), 1360–1374.

<https://doi.org/10.1016/j.cell.2015.11.004>

Choe, A., Ha, S. K., Choi, I., Choi, N., & Sung, J. H. (2017). Microfluidic gut-liver chip for reproducing the first pass metabolism. *Biomedical Microdevices*, *19*(1).

<https://doi.org/10.1007/s10544-016-0143-2>

De Filippo, K., Dudeck, A., Hasenberg, M., Nye, E., van Rooijen, N., Hartmann, K., Gunzer, M., Roers, A., & Hogg, N. (2013). Mast cell and macrophage chemokines CXCL1/CXCL2 control the early stage of neutrophil recruitment during tissue

inflammation. *Blood*, *121*(24), 4930–4937. <https://doi.org/10.1182/blood-2013-02-486217>

DeGruttola, A. K., Low, D., Mizoguchi, A., & Mizoguchi, E. (2016). Current

understanding of dysbiosis in disease in human and animal models. *Inflammatory*

*Bowel Diseases*, 22(5), 1137–1150.

<https://doi.org/10.1097/mib.0000000000000750>

Dobin A, Davis CA, Schlesinger F, Drenkow J, Zaleski C, Jha S, Batut P, Chaisson M, Gingeras TR. STAR: ultrafast universal RNA-seq aligner. *Bioinformatics*. 2013 Jan 1;29(1):15-21. doi: 10.1093/bioinformatics/bts635. Epub 2012 Oct 25. PMID: 23104886; PMCID: PMC3530905.

Donaldson, G. P., Lee, S. M., & Mazmanian, S. K. (2015). Gut biogeography of the bacterial microbiota. *Nature Reviews Microbiology*, 14(1), 20–32.  
<https://doi.org/10.1038/nrmicro3552>

Fallani, M., Young, D., Scott, J., Norin, E., Amarri, S., Adam, R., Aguilera, M., Khanna, S., Gil, A., Edwards, C. A., & Doré, J. (2010). Intestinal Microbiota of 6-week-old infants across Europe: Geographic influence beyond delivery mode, breast-feeding, and antibiotics. *Journal of Pediatric Gastroenterology and Nutrition*, 51(1), 77–84.  
<https://doi.org/10.1097/mpg.0b013e3181d1b11e>

Fetah, K. L., DiPardo, B. J., Kongadzem, E., Tomlinson, J. S., Elzagheid, A., Elmusrati, M., Khademhosseini, A., & Ashammakhi, N. (2019). Cancer modeling-on-a-chip with future Artificial Intelligence Integration. *Small*, 15(50).  
<https://doi.org/10.1002/sml.201901985>

Fouhy, F., Guinane, C. M., Hussey, S., Wall, R., Ryan, C. A., Dempsey, E. M., Murphy, B., Ross, R. P., Fitzgerald, G. F., Stanton, C., & Cotter, P. D. (2012). High-throughput sequencing reveals the incomplete, short-term recovery of infant gut

microbiota following parenteral antibiotic treatment with ampicillin and gentamicin. *Antimicrobial Agents and Chemotherapy*, 56(11), 5811–5820.

<https://doi.org/10.1128/aac.00789-12>

Gleeson, J. P., Fein, K. C., Chaudhary, N., Doerfler, R., Newby, A. N., & Whitehead, K. A. (2021). The enhanced intestinal permeability of infant mice enables oral protein and macromolecular absorption without delivery technology. *International Journal of Pharmaceutics*, 593, 120120. <https://doi.org/10.1016/j.ijpharm.2020.120120>

Guarner, F., & Malagelada, J.-R. (2003). Gut Flora in health and disease. *The Lancet*, 361(9356), 512–519. [https://doi.org/10.1016/s0140-6736\(03\)12489-0](https://doi.org/10.1016/s0140-6736(03)12489-0)

Guinane, C. M., & Cotter, P. D. (2013). Role of the gut microbiota in health and chronic gastrointestinal disease: Understanding a hidden metabolic organ. *Therapeutic Advances in Gastroenterology*, 6(4), 295–308.

<https://doi.org/10.1177/1756283x13482996>

Guo, X.-K., Ou, J., Liang, S., Zhou, X., & Hu, X. (2018). Epithelial HES1 maintains gut homeostasis by preventing microbial dysbiosis. *Mucosal Immunology*, 11(3), 716–726. <https://doi.org/10.1038/mi.2017.111>

He, J., Zhang, P., Shen, L., Niu, L., Tan, Y., Chen, L., Zhao, Y., Bai, L., Hao, X., Li, X., Zhang, S., & Zhu, L. (2020). Short-chain fatty acids and their association with signalling pathways in inflammation, glucose and lipid metabolism. *International Journal of Molecular Sciences*, 21(17), 6356.

<https://doi.org/10.3390/ijms21176356>

- Hemarajata, P., & Versalovic, J. (2012). Effects of probiotics on gut microbiota: Mechanisms of intestinal immunomodulation and neuromodulation. *Therapeutic Advances in Gastroenterology*, 6(1), 39–51.  
<https://doi.org/10.1177/1756283x12459294>
- Hillman, E. T., Lu, H., Yao, T., & Nakatsu, C. H. (2017). Microbial Ecology along the gastrointestinal tract. *Microbes and Environments*, 32(4), 300–313.  
<https://doi.org/10.1264/jsme2.me17017>
- Hou, K., Wu, Z.-X., Chen, X.-Y., Wang, J.-Q., Zhang, D., Xiao, C., Zhu, D., Koya, J. B., Wei, L., Li, J., & Chen, Z.-S. (2022). Microbiota in health and diseases. *Signal Transduction and Targeted Therapy*, 7(1). <https://doi.org/10.1038/s41392-022-00974-4>
- Huh, D., Leslie, D. C., Matthews, B. D., Fraser, J. P., Jurek, S., Hamilton, G. A., Thorneloe, K. S., McAlexander, M. A., & Ingber, D. E. (2012). A human disease model of drug toxicity–induced pulmonary edema in a lung-on-a-chip microdevice. *Science Translational Medicine*, 4(159).  
<https://doi.org/10.1126/scitranslmed.3004249>
- Huus, K. E., & Ley, R. E. (2021). Blowing hot and cold: Body temperature and the microbiome. *mSystems*, 6(5). <https://doi.org/10.1128/msystems.00707-21>
- Iatcu, C. O., Steen, A., & Covasa, M. (2021). Gut microbiota and complications of type-2 diabetes. *Nutrients*, 14(1), 166. <https://doi.org/10.3390/nu14010166>

- Ingber, D. E. (2022). Human organs-on-chips for disease modelling, drug development and Personalized Medicine. *Nature Reviews Genetics*, 23(8), 467–491.  
<https://doi.org/10.1038/s41576-022-00466-9>
- Kasendra, M., Tovaglieri, A., Sontheimer-Phelps, A., Jalili-Firoozinezhad, S., Bein, A., Chalkiadaki, A., Scholl, W., Zhang, C., Rickner, H., Richmond, C. A., Li, H., Breault, D. T., & Ingber, D. E. (2018). Development of a primary human small intestine-on-a-chip using biopsy-derived organoids. *Scientific Reports*, 8(1).  
<https://doi.org/10.1038/s41598-018-21201-7>
- Langdon, A., Crook, N., & Dantas, G. (2016). The effects of antibiotics on the microbiome throughout development and alternative approaches for therapeutic modulation. *Genome Medicine*, 8(1). <https://doi.org/10.1186/s13073-016-0294-z>
- Larsen, N., Vogensen, F. K., van den Berg, F. W., Nielsen, D. S., Andreasen, A. S., Pedersen, B. K., Al-Soud, W. A., Sørensen, S. J., Hansen, L. H., & Jakobsen, M. (2010). Gut microbiota in human adults with type 2 diabetes differs from non-diabetic adults. *PLoS ONE*, 5(2). <https://doi.org/10.1371/journal.pone.0009085>
- LeBlanc, J. G., Milani, C., de Giori, G. S., Sesma, F., van Sinderen, D., & Ventura, M. (2013). Bacteria as vitamin suppliers to their host: A gut microbiota perspective. *Current Opinion in Biotechnology*, 24(2), 160–168.  
<https://doi.org/10.1016/j.copbio.2012.08.005>
- Lambert, G. P., Gisolfi, C. V., Berg, D. J., Moseley, P. L., Oberley, L. W., & Kregel, K. C. (2002). Selected contribution: Hyperthermia-induced intestinal permeability and

the role of oxidative and Nitrosative Stress. *Journal of Applied Physiology*, 92(4), 1750–1761. <https://doi.org/10.1152/jappphysiol.00787.2001>

Lee, B. J., & Bak, Y.-T. (2011). Irritable bowel syndrome, gut microbiota and probiotics. *Journal of Neurogastroenterology and Motility*, 17(3), 252–266. <https://doi.org/10.5056/jnm.2011.17.3.252>

Lee, C. S., & Leong, K. W. (2020). Advances in microphysiological blood-brain barrier (BBB) models towards drug delivery. *Current Opinion in Biotechnology*, 66, 78–87. <https://doi.org/10.1016/j.copbio.2020.06.009>

Lefebvre, P., Cariou, B., Lien, F., Kuipers, F., & Staels, B. (2009). Role of bile acids and bile acid receptors in metabolic regulation. *Physiological Reviews*, 89(1), 147–191. <https://doi.org/10.1152/physrev.00010.2008>

Lennox-King, S., O’Farrell, S., Bettelheim, K., & Shooter, R. (1976). *Escherichia coli* isolated from babies delivered by caesarean section and their environment. *Infection*, 4(3), 139–145. <https://doi.org/10.1007/bf01638940>

Lessa, F. C., Mu, Y., Bamberg, W. M., Beldavs, Z. G., Dumyati, G. K., Dunn, J. R., Farley, M. M., Holzbauer, S. M., Meek, J. I., Phipps, E. C., Wilson, L. E., Winston, L. G., Cohen, J. A., Limbago, B. M., Fridkin, S. K., Gerding, D. N., & McDonald, L. C. (2015). Burden of *clostridium difficile* infection in the United States. *New England Journal of Medicine*, 372(9), 825–834. <https://doi.org/10.1056/nejmoa1408913>

- Ley, R. E., Bäckhed, F., Turnbaugh, P., Lozupone, C. A., Knight, R. D., & Gordon, J. I. (2005). Obesity alters gut microbial ecology. *Proceedings of the National Academy of Sciences*, *102*(31), 11070–11075. <https://doi.org/10.1073/pnas.0504978102>
- Ley, R. E., Turnbaugh, P. J., Klein, S., & Gordon, J. I. (2006). Human gut microbes associated with obesity. *Nature*, *444*(7122), 1022–1023. <https://doi.org/10.1038/4441022a>
- Li, H., Qi, J., & Li, L. (2019). Phytochemicals as potential candidates to combat obesity via adipose non-shivering thermogenesis. *Pharmacological Research*, *147*, 104393. <https://doi.org/10.1016/j.phrs.2019.104393>
- Li, J., Sung, C. Y., Lee, N., Ni, Y., Pihlajamäki, J., Panagiotou, G., & El-Nezami, H. (2016). Probiotics modulated gut microbiota suppresses hepatocellular carcinoma growth in mice. *Proceedings of the National Academy of Sciences*, *113*(9). <https://doi.org/10.1073/pnas.1518189113>
- Longstreth, G. F., Thompson, W. G., Chey, W. D., Houghton, L. A., Mearin, F., & Spiller, R. C. (2006). Functional bowel disorders. *Gastroenterology*, *130*(5), 1480–1491. <https://doi.org/10.1053/j.gastro.2005.11.061>
- Louis, P., & Flint, H. J. (2016). Formation of propionate and butyrate by the human colonic microbiota. *Environmental Microbiology*, *19*(1), 29–41. <https://doi.org/10.1111/1462-2920.13589>

- Love MI, Huber W, Anders S (2014). “Moderated estimation of fold change and dispersion for RNA-seq data with DESeq2.” *Genome Biology*, **15**, 550. [doi:10.1186/s13059-014-0550-8](https://doi.org/10.1186/s13059-014-0550-8).
- Lozupone, C. A., Stombaugh, J. I., Gordon, J. I., Jansson, J. K., & Knight, R. (2012). Diversity, stability and resilience of the human gut microbiota. *Nature*, *489*(7415), 220–230. <https://doi.org/10.1038/nature11550>
- Ma, J., Li, Z., Zhang, W., Zhang, C., Zhang, Y., Mei, H., Zhuo, N., Wang, H., Wang, L., & Wu, D. (2020). Comparison of gut microbiota in exclusively breast-fed and formula-fed babies: A study of 91 term infants. *Scientific Reports*, *10*(1). <https://doi.org/10.1038/s41598-020-72635-x>
- Mazmanian, S. K., Liu, C. H., Tzianabos, A. O., & Kasper, D. L. (2005). An immunomodulatory molecule of symbiotic bacteria directs maturation of the host immune system. *Cell*, *122*(1), 107–118. <https://doi.org/10.1016/j.cell.2005.05.007>
- Mills, S., Shanahan, F., Stanton, C., Hill, C., Coffey, A., & Ross, R. P. (2013). Movers and shakers. *Gut Microbes*, *4*(1), 4–16. <https://doi.org/10.4161/gmic.22371>
- Morad, G., Carman, C. V., Hagedorn, E. J., Perlin, J. R., Zon, L. I., Mustafaoglu, N., Park, T.-E., Ingber, D. E., Daisy, C. C., & Moses, M. A. (2019). Tumor-derived extracellular vesicles breach the intact blood–brain barrier *viatranscytosis*. *ACS Nano*, *13*(12), 13853–13865. <https://doi.org/10.1021/acsnano.9b04397>



Morrison, D. J., & Preston, T. (2016). Formation of short chain fatty acids by the gut microbiota and their impact on human metabolism. *Gut Microbes*, 7(3), 189–200.

<https://doi.org/10.1080/19490976.2015.1134082>

Mullish, B. H., & Williams, H. R. (2018). *clostridium difficile* infection and antibiotic-associated diarrhoea. *Clinical Medicine*, 18(3), 237–241.

<https://doi.org/10.7861/clinmedicine.18-3-237>

Na, J. Y., Park, J. M., Lee, K. S., Kang, J. O., Oh, S. H., & Kim, Y. J. (2014). Clinical characteristics of symptomatic *clostridium difficile* infection in children: Conditions as infection risks and whether probiotics is effective. *Pediatric Gastroenterology, Hepatology & Nutrition*, 17(4), 232.

<https://doi.org/10.5223/pghn.2014.17.4.232>

National Academies of Sciences, Engineering, and Medicine; Division on Earth and Life Studies; Board on Life Sciences; Board on Environmental Studies and Toxicology; Committee on Advancing Understanding of the Implications of Environmental-Chemical Interactions with the Human Microbiome. Environmental Chemicals, the Human Microbiome, and Health Risk: A Research Strategy. Washington (DC): National Academies Press (US); 2017 Dec 29. 4, Current Methods for Studying the Human Microbiome. Available from:

<https://www.ncbi.nlm.nih.gov/books/NBK481559/>

- Nguyen, T. L., Vieira-Silva, S., Liston, A., & Raes, J. (2015). How informative is the mouse for human gut microbiota research? *Disease Models & Mechanisms*, 8(1), 1–16. <https://doi.org/10.1242/dmm.017400>
- Ogden, H. B., Fallowfield, J. L., Child, R. B., Davison, G., Fleming, S. C., Edinburgh, R. M., Delves, S. K., Millyard, A., Westwood, C. S., & Layden, J. D. (2020). Reliability of gastrointestinal barrier integrity and microbial translocation biomarkers at rest and following exertional heat stress. *Physiological Reports*, 8(5). <https://doi.org/10.14814/phy2.14374>
- Ogobuiro I, Gonzales J, Shumway KR, Tuma F. Physiology, Gastrointestinal. 2023 Apr 8. In: StatPearls [Internet]. Treasure Island (FL): StatPearls Publishing; 2024 Jan—. PMID: 30725788.
- Ohio Supercomputer Center. 1987. Ohio Supercomputer Center. Columbus OH: Ohio Supercomputer Center. <http://osc.edu/ark:/19495/f5s1ph73>.
- Panda, S., El khader, I., Casellas, F., López Vivancos, J., García Cors, M., Santiago, A., Cuenca, S., Guarner, F., & Manichanh, C. (2014). Short-term effect of antibiotics on human gut microbiota. *PLoS ONE*, 9(4). <https://doi.org/10.1371/journal.pone.0095476>
- Park, T.-E., Mustafaoglu, N., Herland, A., Hasselkus, R., Mannix, R., FitzGerald, E. A., Prantil-Baun, R., Watters, A., Henry, O., Benz, M., Sanchez, H., McCrea, H. J., Goumnerova, L. C., Song, H. W., Palecek, S. P., Shusta, E., & Ingber, D. E. (2019). Hypoxia-enhanced blood-brain barrier chip recapitulates human barrier function

and shuttling of drugs and antibodies. *Nature Communications*, 10(1).

<https://doi.org/10.1038/s41467-019-10588-0>

Pasquier, M., Carron, P. N., Rodrigues, A., Dami, F., Frochoux, V., Sartori, C.,

Deslarzes, T., & Rousson, V. (2019). An evaluation of the Swiss staging model for hypothermia using hospital cases and case reports from the literature. *Scandinavian Journal of Trauma, Resuscitation and Emergency Medicine*, 27(1).

<https://doi.org/10.1186/s13049-019-0636-0>

Payne, A. N., Chassard, C., Zimmermann, M., Müller, P., Stinca, S., & Lacroix, C.

(2011). The metabolic activity of gut microbiota in obese children is increased compared with normal-weight children and exhibits more exhaustive substrate utilization. *Nutrition & Diabetes*, 1(7). <https://doi.org/10.1038/nutd.2011.8>

Pediaditakis, I., Kodella, K. R., Manatakis, D. V., Le, C. Y., Hinojosa, C. D., Tien-Street,

W., Manolagos, E. S., Vekrellis, K., Hamilton, G. A., Ewart, L., Rubin, L. L., & Karalis, K. (2021). Modeling alpha-synuclein pathology in a human brain-chip to assess blood-brain barrier disruption. *Nature Communications*, 12(1).

<https://doi.org/10.1038/s41467-021-26066-5>

Penders, J., Thijs, C., Vink, C., Stelma, F. F., Snijders, B., Kummeling, I., van den

Brandt, P. A., & Stobberingh, E. E. (2006). Factors influencing the composition of the intestinal microbiota in early infancy. *Pediatrics*, 118(2), 511–521.

<https://doi.org/10.1542/peds.2005-2824>

Peng, M., Yi, W., Murong, M., Peng, N., Tong, H., Jiang, M., Jin, D., Peng, S., Liang, W., Quan, J., Li, M., Shi, L., & Xiao, G. (2023). Akkermansia muciniphila improves heat stress-impaired intestinal barrier function by modulating HSP27 in Caco-2 cells. *Microbial Pathogenesis*, 177, 106028.

<https://doi.org/10.1016/j.micpath.2023.106028>

Pradhan, R., Ngo, P. A., Martínez-Sánchez, L. d., Neurath, M. F., & López-Posadas, R. (2021). Rho GTPases as key molecular players within intestinal mucosa and GI diseases. *Cells*, 10(1), 66. <https://doi.org/10.3390/cells10010066>

Qu, J., Ko, C.-W., Tso, P., & Bhargava, A. (2019). Apolipoprotein A-IV: A multifunctional protein involved in protection against atherosclerosis and diabetes. *Cells*, 8(4), 319. <https://doi.org/10.3390/cells8040319>

Quévrain, E., Maubert, M. A., Michon, C., Chain, F., Marquant, R., Tailhades, J., Miquel, S., Carlier, L., Bermúdez-Humarán, L. G., Pigneur, B., Lequin, O., Kharrat, P., Thomas, G., Rainteau, D., Aubry, C., Breyner, N., Afonso, C., Lavielle, S., Grill, J.-P., ... Seksik, P. (2015). Identification of an anti-inflammatory protein from *faecalibacterium prausnitzii*, a commensal bacterium deficient in crohn's disease. *Gut*, 65(3), 415–425. <https://doi.org/10.1136/gutjnl-2014-307649>

R Core Team (2021). R: A language and environment for statistical computing. R Foundation for Statistical Computing, Vienna, Austria. URL <https://www.R-project.org/>.

- Rousset, X., Shamburek, R., Vaisman, B., Amar, M., & Remaley, A. T. (2011). Lecithin cholesterol acyltransferase: An anti- or pro-atherogenic factor? *Current Atherosclerosis Reports*, *13*(3), 249–256. <https://doi.org/10.1007/s11883-011-0171-6>
- Rutayisire, E., Huang, K., Liu, Y., & Tao, F. (2016). The mode of delivery affects the diversity and colonization pattern of the gut microbiota during the first year of infants' life: A systematic review. *BMC Gastroenterology*, *16*(1). <https://doi.org/10.1186/s12876-016-0498-0>
- Schwab, F., Gastmeier, P., Hoffmann, P., & Meyer, E. (2020). Summer, Sun and sepsis—the influence of outside temperature on nosocomial bloodstream infections: A cohort study and review of the literature. *PLOS ONE*, *15*(6). <https://doi.org/10.1371/journal.pone.0234656>
- Schwartz, A., Taras, D., Schäfer, K., Beijer, S., Bos, N. A., Donus, C., & Hardt, P. D. (2010). Microbiota and SCFA in lean and overweight healthy subjects. *Obesity*, *18*(1), 190–195. <https://doi.org/10.1038/oby.2009.167>
- Segain, J.-P. (2000). Butyrate inhibits inflammatory responses through nfkappa B inhibition: Implications for crohn's disease. *Gut*, *47*(3), 397–403. <https://doi.org/10.1136/gut.47.3.397>
- Sekirov, I., Tam, N. M., Jogova, M., Robertson, M. L., Li, Y., Lupp, C., & Finlay, B. B. (2008). Antibiotic-induced perturbations of the intestinal microbiota alter host

susceptibility to enteric infection. *Infection and Immunity*, 76(10), 4726–4736.

<https://doi.org/10.1128/iai.00319-08>

Sender, R., Fuchs, S., & Milo, R. (2016). Revised estimates for the number of human and bacteria cells in the body. *PLOS Biology*, 14(8).

<https://doi.org/10.1371/journal.pbio.1002533>

Sontheimer-Phelps, A., Chou, D. B., Tovaglieri, A., Ferrante, T. C., Duckworth, T., Fadel, C., Frisimantas, V., Sutherland, A. D., Jalili-Firoozinezhad, S., Kasendra, M., Stas, E., Weaver, J. C., Richmond, C. A., Levy, O., Prantil-Baun, R., Breault, D. T., & Ingber, D. E. (2020). Human colon-on-a-chip enables continuous in vitro analysis of colon mucus layer accumulation and physiology. *Cellular and Molecular Gastroenterology and Hepatology*, 9(3), 507–526.

<https://doi.org/10.1016/j.jcmgh.2019.11.008>

Staley, C., Weingarden, A. R., Khoruts, A., & Sadowsky, M. J. (2016). Interaction of gut microbiota with bile acid metabolism and its influence on disease states. *Applied Microbiology and Biotechnology*, 101(1), 47–64. <https://doi.org/10.1007/s00253-016-8006-6>

STEINMETZ, A., KAFFARNIK, H., & UTERMANN, G. (1985). Activation of phosphatidylcholine–sterol acyltransferase by human apolipoprotein E isoforms. *European Journal of Biochemistry*, 152(3), 747–751.

<https://doi.org/10.1111/j.1432-1033.1985.tb09256.x>

Structure, function and diversity of the healthy human microbiome. Human Microbiome Project Consortium, *Nature*, 486 (2012)\ , pp. 207–214

Tanaka T, Narazaki M, Kishimoto T. IL-6 in inflammation, immunity, and disease. *Cold Spring Harb Perspect Biol.* 2014 Sep 4;6(10):a016295. doi: 10.1101/cshperspect.a016295. PMID: 25190079; PMCID: PMC4176007.

Thursby, E., & Juge, N. (2017). Introduction to the human gut microbiota. *Biochemical Journal*, 474(11), 1823–1836. <https://doi.org/10.1042/bcj20160510>

Trujillo-de Santiago, G., Flores-Garza, B. G., Tavares-Negrete, J. A., Lara-Mayorga, I. M., González-Gamboa, I., Zhang, Y. S., Rojas-Martínez, A., Ortiz-López, R., & Álvarez, M. M. (2019). The tumor-on-chip: Recent advances in the development of microfluidic systems to recapitulate the physiology of solid tumors. *Materials*, 12(18), 2945. <https://doi.org/10.3390/ma12182945>

U.S. National Library of Medicine. (n.d.). *Rhov Ras homolog family member V [Homo Sapiens (human)] - gene - NCBI*. National Center for Biotechnology Information. <https://www.ncbi.nlm.nih.gov/gene/171177>

Valdes, A. M., Walter, J., Segal, E., & Spector, T. D. (2018). Role of the gut microbiota in nutrition and health. *BMJ*. <https://doi.org/10.1136/bmj.k2179>

Vyas, U., & Ranganathan, N. (2012). Probiotics, prebiotics, and synbiotics: Gut and beyond. *Gastroenterology Research and Practice*, 2012, 1–16. <https://doi.org/10.1155/2012/872716>

Wang F, Kohan AB, Lo CM, Liu M, Howles P, Tso P. Apolipoprotein A-IV: a protein intimately involved in metabolism. *J Lipid Res.* 2015 Aug;56(8):1403-18. doi: 10.1194/jlr.R052753. Epub 2015 Feb 1. PMID: 25640749; PMCID: PMC4513983.

Whitesides, G. M. (2006). The origins and the future of Microfluidics. *Nature*, 442(7101), 368–373. <https://doi.org/10.1038/nature05058>

Wiertsema, S. P., van Bergenhenegouwen, J., Garssen, J., & Knippels, L. M. (2021). The interplay between the gut microbiome and the immune system in the context of infectious diseases throughout life and the role of Nutrition in Optimizing Treatment Strategies. *Nutrients*, 13(3), 886. <https://doi.org/10.3390/nu13030886>

Yatsunenko, T., Rey, F. E., Manary, M. J., Trehan, I., Dominguez-Bello, M. G., Contreras, M., Magris, M., Hidalgo, G., Baldassano, R. N., Anokhin, A. P., Heath, A. C., Warner, B., Reeder, J., Kuczynski, J., Caporaso, J. G., Lozupone, C. A., Lauber, C., Clemente, J. C., Knights, D., ... Gordon, J. I. (2012). Human gut microbiome viewed across age and geography. *Nature*, 486(7402), 222–227. <https://doi.org/10.1038/nature11053>

Yoon, M. Y., & Yoon, S. S. (2018). Disruption of the gut ecosystem by antibiotics. *Yonsei Medical Journal*, 59(1), 4. <https://doi.org/10.3349/ymj.2018.59.1.4>

Zhang, X., Zhang, S., Wang, C., Wang, B., & Guo, P. (2014). Effects of moderate strength cold air exposure on blood pressure and biochemical indicators among cardiovascular and cerebrovascular patients. *International Journal of*



*Environmental Research and Public Health*, 11(3), 2472–2487.

<https://doi.org/10.3390/ijerph110302472>